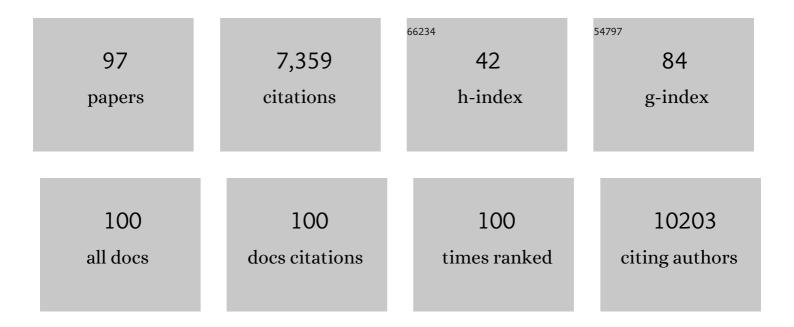
List of Publications by Year in descending order

Source: https://exaly.com/author-pdf/5416053/publications.pdf Version: 2024-02-01



#	Article	IF	CITATIONS
1	Structural origin of low Li-ion conductivity in perovskite solid-state electrolyte. Nano Energy, 2022, 92, 106758.	8.2	18
2	Balancing the film strain of organic semiconductors for ultrastable organic transistors with a five-year lifetime. Nature Communications, 2022, 13, 1480.	5.8	26
3	Structural Heterogeneity Induced Li Dendrite Growth in Li _{0.33} La _{0.56} TiO ₃ Solid-State Electrolytes. ACS Applied Energy Materials, 2022, 5, 3741-3747.	2.5	6
4	A Hollow Porous Metalâ€Organic Framework Enabled Polyethylene Oxide Based Composite Polymer Electrolytes for Allâ€Solidâ€State Lithium Batteries. Batteries and Supercaps, 2022, 5, .	2.4	6
5	Comparative study of oxide-derived Cu electrocatalysts through electrochemical vs. thermal reduction. Chemical Communications, 2022, 58, 6120-6123.	2.2	3
6	Atomic Defect Mediated Li-Ion Diffusion in a Lithium Lanthanum Titanate Solid-State Electrolyte. ACS Nano, 2022, 16, 6898-6905.	7.3	7
7	Improving the cyclability of solid polymer electrolyte with porous V2O5 nanotube filler. Materials Today Energy, 2022, 28, 101062.	2.5	7
8	Revealing synergetic structural activation of a CuAu surface during water–gas shift reaction. Proceedings of the National Academy of Sciences of the United States of America, 2022, 119, .	3.3	5
9	Enhancing Li-ion conduction in composite polymer electrolytes using Li _{0.33} La _{0.56} TiO ₃ nanotubes. Chemical Communications, 2021, 57, 11068-11071.	2.2	6
10	Effect of surface steps on chemical ordering in the subsurface of Cu(Au) solid solutions. Physical Review B, 2021, 103, .	1.1	5
11	N8 stabilized single-atom Pd for highly selective hydrogenation of acetylene. Journal of Catalysis, 2021, 395, 46-53.	3.1	16
12	In situ monitoring nanoscale solid-state phase transformation of Ag nanowire during electrochemical reaction. Scripta Materialia, 2021, 199, 113835.	2.6	1
13	Atomic-Scale Interfacial Phase Transformation Governed Cu Oxidation in Water Vapor. Journal of Physical Chemistry Letters, 2021, 12, 6996-7001.	2.1	2
14	Structural Evolution of Cu/ZnO Catalysts during Water-Gas Shift Reaction: An <i>In Situ</i> Transmission Electron Microscopy Study. ACS Applied Materials & Interfaces, 2021, 13, 41707-41714.	4.0	17
15	Labile Fe(III) supersaturation controls nucleation and properties of product phases from Fe(II)-catalyzed ferrihydrite transformation. Geochimica Et Cosmochimica Acta, 2021, 309, 272-285.	1.6	24
16	Defect-driven selective metal oxidation at atomic scale. Nature Communications, 2021, 12, 558.	5.8	47
17	Atomic Scale Mechanisms of Multimode Oxide Growth on Nickel–Chromium Alloy: Direct <i>In Situ</i> Observation of the Initial Oxide Nucleation and Growth. ACS Applied Materials & Interfaces, 2021, 13, 1903-1913.	4.0	8
18	Gas adsorbate-induced Au atomic segregation and clustering from Cu(Au). Science China Materials, 2021, 64, 1256-1266.	3.5	2

#	Article	IF	CITATIONS
19	Realâ€Time Atomicâ€Scale Visualization of Reversible Copper Surface Activation during the CO Oxidation Reaction. Angewandte Chemie - International Edition, 2020, 59, 2505-2509.	7.2	24
20	Realâ€Time Atomicâ€Scale Visualization of Reversible Copper Surface Activation during the CO Oxidation Reaction. Angewandte Chemie, 2020, 132, 2526-2530.	1.6	11
21	Atomic-Scale Dynamic Interaction of <mml:math xmins:mml="http://www.w3.org/1998/Math/Math/Math/Math/Math/Math/Math/Math</td"><td>)>₂ınıl:m</td><td>i 11</td></mml:math>)> ₂ı nıl:m	i 11
22	Stress-resilient electrode materials for lithium-ion batteries: strategies and mechanisms. Chemical Communications, 2020, 56, 13301-13312.	2.2	13
23	Electrolyte-Phobic Surface for the Next-Generation Nanostructured Battery Electrodes. Nano Letters, 2020, 20, 7455-7462.	4.5	25
24	Atomic-scale phase separation induced clustering of solute atoms. Nature Communications, 2020, 11, 3934.	5.8	11
25	Direct Visualization of Atomic-Scale Graphene Growth on Cu through Environmental Transmission Electron Microscopy. ACS Applied Materials & Interfaces, 2020, 12, 52201-52207.	4.0	9
26	Vacancy ordering during selective oxidation of β-NiAl. Materialia, 2020, 12, 100783.	1.3	6
27	Hierarchical porous silicon structures with extraordinary mechanical strength as high-performance lithium-ion battery anodes. Nature Communications, 2020, 11, 1474.	5.8	298
28	Direct visualization of dynamic atomistic processes of Cu2O crystal growth through gas-solid reaction. Nano Energy, 2020, 70, 104527.	8.2	12
29	Dynamic Atom Clusters on AuCu Nanoparticle Surface during CO Oxidation. Journal of the American Chemical Society, 2020, 142, 4022-4027.	6.6	36
30	Deciphering atomistic mechanisms of the gas-solid interfacial reaction during alloy oxidation. Science Advances, 2020, 6, eaay8491.	4.7	20
31	Electrocatalytic Hydrogen Evolution in Neutral pH Solutions: Dual-Phase Synergy. ACS Catalysis, 2019, 9, 8712-8718.	5.5	103
32	Atomic-scale combination of germanium-zinc nanofibers for structural and electrochemical evolution. Nature Communications, 2019, 10, 2364.	5.8	44
33	Self-smoothing anode for achieving high-energy lithium metal batteries under realistic conditions. Nature Nanotechnology, 2019, 14, 594-601.	15.6	451
34	Highly Stable Oxygen Electrodes Enabled by Catalyst Redistribution through an In Situ Electrochemical Method. Advanced Energy Materials, 2019, 9, 1803598.	10.2	6
35	Minimized Volume Expansion in Hierarchical Porous Silicon upon Lithiation. ACS Applied Materials & Interfaces, 2019, 11, 13257-13263.	4.0	51
36	High performance porous Si@C anodes synthesized by low temperature aluminothermic reaction. Electrochimica Acta, 2018, 269, 509-516.	2.6	51

#	Article	IF	CITATIONS
37	Harnessing the concurrent reaction dynamics in active Si and Ge to achieve high performance lithium-ion batteries. Energy and Environmental Science, 2018, 11, 669-681.	15.6	329
38	Revealing the Reaction Mechanism of Na–O ₂ Batteries using Environmental Transmission Electron Microscopy. ACS Energy Letters, 2018, 3, 393-399.	8.8	30
39	In-Situ S/TEM Probing of the Behavior of Nanoparticles Under Chemical and Electrochemical Reactions in the System Involving Solid, Liquid and Gas. Microscopy and Microanalysis, 2018, 24, 1876-1877.	0.2	4
40	In Situ Transmission Electron Microsopy of Oxide Shell-Induced Pore Formation in (De)lithiated Silicon Nanowires. ACS Energy Letters, 2018, 3, 2829-2834.	8.8	25
41	A novel approach to synthesize micrometer-sized porous silicon as a high performance anode for lithium-ion batteries. Nano Energy, 2018, 50, 589-597.	8.2	191
42	Coupling of electrochemically triggered thermal and mechanical effects to aggravate failure in a layered cathode. Nature Communications, 2018, 9, 2437.	5.8	200
43	Tailoring the formation of textured oxide films via primary and secondary nucleation of oxide islands. Acta Materialia, 2018, 156, 266-274.	3.8	2
44	Stress-Tolerant Nanoporous Germanium Nanofibers for Long Cycle Life Lithium Storage with High Structural Stability. ACS Nano, 2018, 12, 8169-8176.	7.3	42
45	Mechanical mismatch-driven rippling in carbon-coated silicon sheets for stress-resilient battery anodes. Nature Communications, 2018, 9, 2924.	5.8	94
46	Size-dependent dynamic structures of supported gold nanoparticles in CO oxidation reaction condition. Proceedings of the National Academy of Sciences of the United States of America, 2018, 115, 7700-7705.	3.3	183
47	Atomic origins of water-vapour-promoted alloy oxidation. Nature Materials, 2018, 17, 514-518.	13.3	106
48	B4C as a stable non-carbon-based oxygen electrode material for lithium-oxygen batteries. Nano Energy, 2017, 33, 195-204.	8.2	65
49	Oneâ€Pot Process for Hydrodeoxygenation of Lignin to Alkanes Using Ruâ€Based Bimetallic and Bifunctional Catalysts Supported on Zeolite Y. ChemSusChem, 2017, 10, 1846-1856.	3.6	127
50	Complete Decomposition of Li ₂ CO ₃ in Li–O ₂ Batteries Using Ir/B ₄ C as Noncarbon-Based Oxygen Electrode. Nano Letters, 2017, 17, 1417-1424.	4.5	104
51	Insights on the Mechanism of Na-Ion Storage in Soft Carbon Anode. Chemistry of Materials, 2017, 29, 2314-2320.	3.2	177
52	Direction-specific van der Waals attraction between rutile TiO ₂ nanocrystals. Science, 2017, 356, 434-437.	6.0	103
53	Wide-Temperature Electrolytes for Lithium-Ion Batteries. ACS Applied Materials & Interfaces, 2017, 9, 18826-18835.	4.0	150
54	Revealing the reaction mechanisms of Li–O2 batteries using environmental transmission electron microscopy. Nature Nanotechnology, 2017, 12, 535-539.	15.6	160

#	Article	IF	CITATIONS
55	Revealing the Dynamics of Platinum Nanoparticle Catalysts on Carbon in Oxygen and Water Using Environmental TEM. ACS Catalysis, 2017, 7, 7658-7664.	5.5	38
56	Rock-Salt Growth-Induced (003) Cracking in a Layered Positive Electrode for Li-Ion Batteries. ACS Energy Letters, 2017, 2, 2607-2615.	8.8	116
57	Single Atomic Iron Catalysts for Oxygen Reduction in Acidic Media: Particle Size Control and Thermal Activation. Journal of the American Chemical Society, 2017, 139, 14143-14149.	6.6	1,215
58	Yolk-shell structured Sb@C anodes for high energy Na-ion batteries. Nano Energy, 2017, 40, 504-511.	8.2	123
59	Li ⁺ -Desolvation Dictating Lithium-Ion Battery's Low-Temperature Performances. ACS Applied Materials & Interfaces, 2017, 9, 42761-42768.	4.0	200
60	Nitrogen–doped graphitized carbon shell encapsulated NiFe nanoparticles: A highly durable oxygen evolution catalyst. Nano Energy, 2017, 39, 245-252.	8.2	143
61	In-situ TEM Study of Coating Layer Function on Silicon Anode Particle for Lithium Ion Battery. Microscopy and Microanalysis, 2016, 22, 1324-1325.	0.2	1
62	Electrochemically Formed Ultrafine Metal Oxide Nanocatalysts for High-Performance Lithium–Oxygen Batteries. Nano Letters, 2016, 16, 4932-4939.	4.5	62
63	Atomistic Conversion Reaction Mechanism of WO ₃ in Secondary Ion Batteries of Li, Na, and Ca. Angewandte Chemie - International Edition, 2016, 55, 6244-6247.	7.2	86
64	Highly Reversible Zinc-Ion Intercalation into Chevrel Phase Mo ₆ S ₈ Nanocubes and Applications for Advanced Zinc-Ion Batteries. ACS Applied Materials & Interfaces, 2016, 8, 13673-13677.	4.0	256
65	In Situ and Ex Situ TEM Study of Lithiation Behaviours of Porous Silicon Nanostructures. Scientific Reports, 2016, 6, 31334.	1.6	43
66	Reactions of graphene supported Co ₃ O ₄ nanocubes with lithium and magnesium studied by <i>in situ</i> transmission electron microscopy. Nanotechnology, 2016, 27, 085402.	1.3	15
67	Atomistic Conversion Reaction Mechanism of WO ₃ in Secondary Ion Batteries of Li, Na, and Ca. Angewandte Chemie, 2016, 128, 6352-6355.	1.6	21
68	In situ atomic scale visualization of surface kinetics driven dynamics of oxide growth on a Ni–Cr surface. Chemical Communications, 2016, 52, 3300-3303.	2.2	38
69	In-situ transmission electron microscopy study of surface oxidation for Ni–10Cr and Ni–20Cr alloys. Scripta Materialia, 2016, 114, 129-132.	2.6	43
70	Germanium as a Sodium Ion Battery Material: <i>In Situ</i> TEM Reveals Fast Sodiation Kinetics with High Capacity. Chemistry of Materials, 2016, 28, 1236-1242.	3.2	134
71	Size-Controlled Intercalation-to-Conversion Transition in Lithiation of Transition-Metal Chalcogenides—NbSe ₃ . ACS Nano, 2016, 10, 1249-1255.	7.3	29
72	Suppressing Manganese Dissolution from Lithium Manganese Oxide Spinel Cathodes with Single‣ayer Graphene. Advanced Energy Materials, 2015, 5, 1500646.	10.2	72

#	Article	IF	CITATIONS
73	Reaction Mechanism and Kinetic of Graphene Supported Co3O4 Nanocubes with Lithium and Magnesium Studied by in situ TEM. Microscopy and Microanalysis, 2015, 21, 1197-1198.	0.2	1
74	Nucleation and growth of oxide islands during the initial-stage oxidation of (100)Cu-Pt alloys. Journal of Applied Physics, 2015, 117, .	1.1	10
75	Atomic-Resolution Visualization of Distinctive Chemical Mixing Behavior of Ni, Co, and Mn with Li in Layered Lithium Transition-Metal Oxide Cathode Materials. Chemistry of Materials, 2015, 27, 5393-5401.	3.2	108
76	Surface-Coating Regulated Lithiation Kinetics and Degradation in Silicon Nanowires for Lithium Ion Battery. ACS Nano, 2015, 9, 5559-5566.	7.3	118
77	Post-Assembly Atomic Layer Deposition of Ultrathin Metal-Oxide Coatings Enhances the Performance of an Organic Dye-Sensitized Solar Cell by Suppressing Dye Aggregation. ACS Applied Materials & Interfaces, 2015, 7, 5150-5159.	4.0	43
78	Surface Coating Constraint Induced Self-Discharging of Silicon Nanoparticles as Anodes for Lithium Ion Batteries. Nano Letters, 2015, 15, 7016-7022.	4.5	113
79	Co3O4 nanocubes homogeneously assembled on few-layer graphene for high energy density lithium-ion batteries. Journal of Power Sources, 2015, 274, 816-822.	4.0	164
80	Dynamics of Electrochemical Lithiation/Delithiation of Graphene-Encapsulated Silicon Nanoparticles Studied by In-situ TEM. Scientific Reports, 2014, 4, 3863.	1.6	83
81	Comparative study of the alloying effect on the initial oxidation of Cu-Au(100) and Cu-Pt(100). Applied Physics Letters, 2014, 104, 121601.	1.5	15
82	Atomic Resolution Study of Reversible Conversion Reaction in Metal Oxide Electrodes for Lithium-Ion Battery. ACS Nano, 2014, 8, 11560-11566.	7.3	142
83	Surface-Step-Induced Oscillatory Oxide Growth. Physical Review Letters, 2014, 113, 136104.	2.9	52
84	Tackling Reversible Conversion Reaction Mechanism for Lithium Based Battery. Microscopy and Microanalysis, 2014, 20, 1618-1619.	0.2	4
85	Isotropic to Anisotropic Transition Observed in Si Nanoparticles Lithiation by in situ TEM. Microscopy and Microanalysis, 2014, 20, 1652-1653.	0.2	0
86	10.1063/1.4870085.1., 2014, , .		1
87	Transient Oxidation of Cu-5at.%Ni(001): Temperature Dependent Sequential Oxide Formation. Oxidation of Metals, 2013, 79, 303-311.	1.0	3
88	Dye Stabilization and Enhanced Photoelectrode Wettability in Water-Based Dye-Sensitized Solar Cells through Post-assembly Atomic Layer Deposition of TiO ₂ . Journal of the American Chemical Society, 2013, 135, 11529-11532.	6.6	94
89	In situ atomic-scale visualization of oxide islanding during oxidation of Cu surfaces. Chemical Communications, 2013, 49, 10862.	2.2	54
90	Effect of gold composition on the orientations of oxide nuclei during the early stage oxidation of Cu-Au alloys. Journal of Applied Physics, 2012, 111, 083533.	1.1	10

#	Article	IF	CITATIONS
91	Effect of oxygen gas pressure on orientations of Cu2O nuclei during the initial oxidation of Cu(100), (110) and (111). Surface Science, 2012, 606, 1790-1797.	0.8	28
92	Influence of the surface morphology on the early stages of Cu oxidation. Applied Surface Science, 2012, 259, 791-798.	3.1	4
93	Step-Edge-Induced Oxide Growth During the Oxidation of Cu Surfaces. Physical Review Letters, 2012, 109, 235502.	2.9	103
94	Dependence of degree of orientation of copper oxide nuclei on oxygen pressure during initial stages of copper oxidation. Physical Review B, 2011, 83, .	1.1	17
95	Effect of Oxygen Pressure on the Initial Oxidation Behavior of Cu and Cu-Au Alloys. Materials Research Society Symposia Proceedings, 2011, 1318, 1.	0.1	2
96	Mineralization of flagella for nanotube formation. Materials Science and Engineering C, 2009, 29, 2282-2286.	3.8	21
97	Synthesis of ZnO flowers and their photoluminescence properties. Materials Research Bulletin, 2008, 43, 1883-1891	2.7	48